International Conference on Space Optics—ICSO 2022

Dubrovnik, Croatia

3–7 October 2022

Edited by Kyriaki Minoglou, Nikos Karafolas, and Bruno Cugny,

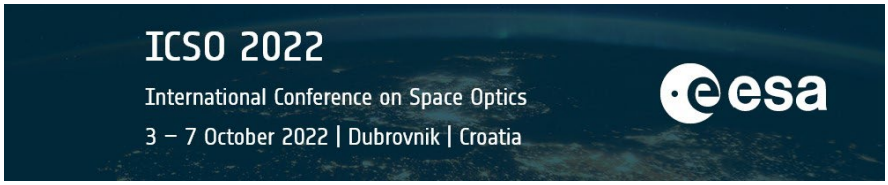

Laser frequency stabilisation for the LISA mission using a cubic cavity

International Conference on Space Optics — ICSO 2022, edited by Kyriaki Minoglou, Nikos Karafolas, Bruno Cugny, Proc. of SPIE Vol. 12777, 127777F · © 2023 ESA and CNES · 0277-786X · doi: 10.1117/12.2691441

Laser frequency stabilisation for the LISA mission using a cubic cavity

Jonathan Stacey, Geoffrey P. Barwood, Alessio Spampinato, Peter Tsoulos, Conor Robinson, Paul Gaynor and Patrick Gill
National Physical Laboratory, Hampton Road, Teddington, Middlesex, TW11 0LW, UK

ABSTRACT

The design and testing of a laser frequency stabilisation system is presented for potential use in the LISA mission. The system is based on a National Physical Laboratory (NPL) dual-axis cubic cavity. The cavity spacer is manufactured from Corning ultra-low expansion (ULE) glass and incorporates thermo-mechanically insensitive mounting to allow compliance to LISA frequency noise power spectral density (PSD) requirements within the ESA-specified thermal and vibration noise environments.

The performance of this cavity-based frequency stabilised laser has been determined by beat frequency comparison versus an NPL optical clock reference cavity. Light is propagated via fibre from this reference laser and an optical path-length stabilisation system is implemented to cancel phase noise induced in the fibre link. We have measured the thermal expansion for both axes of the cube and control the temperature where the linear thermal expansion of one bore is near zero. We have also measured the contribution to the overall frequency stability of thermal noise in a proposed 5-m fibre link between the laser and cavity. Finally, we demonstrate that a laser locked to the NPL cubic cavity meets the LISA frequency noise requirements.

Keywords: optical cavities, laser frequency stabilization, LISA, thermal noise

1. INTRODUCTION

We present work undertaken at the UK National Physical Laboratory (NPL) on the design and testing of a laser frequency stabilisation system for potential use in the LISA mission. The system is based on the NPL dual axis cubic cavity [1, 2] (DACC), implemented to TRL4 within this project (although TRL6 is already achieved for the single axis case [3]). The cavity spacer is manufactured from Corning ultra-low expansion (ULE) glass with a zero linear thermal expansion coefficient specified to lie in the temperature range 25 °C to 35 °C. The design incorporates thermo-mechanically insensitive mounting including multiple thermal shrouds to allow compliance to LISA frequency noise power spectral density (PSD) requirements within the ESA-specified thermal and vibration noise environments.

Frequency control of a commercial 1064 nm laser to a dual-axis cubic cavity is achieved using Pound-Drever-Hall locking via NPL-designed electronics. Two optical axes along two of the three orthogonal bores of the spacer have a measured finesse of more than 200,000. The performance of this cavity-based frequency stabilised laser has been determined by beat frequency comparison versus an NPL optical clock master oscillator cavity housed within a separate laboratory at NPL. Light is propagated via fibre from this reference laser and an optical path-length stabilisation system is implemented to cancel phase noise induced in the fibre link.

The LISA frequency noise power spectral density requirement (in units of Hz/√Hz) is given over the frequency range 0.1 mHz $\leq f \leq$ 1 Hz by:

$$\sqrt{S_\nu(f)} \leq 30 \frac{Hz}{\sqrt{Hz}} \sqrt{1 + \left(\frac{2\,mHz}{f}\right)^4} \quad (1)$$

This frequency noise specification needs to be met where the thermal noise at the boundary in K/√Hz is given by:

$$\sqrt{S_T(f)} = 0.1\frac{K}{\sqrt{Hz}}\sqrt{1+\left(\frac{20\ mHz}{f}\right)^4} \quad (2)$$

In the following sections we explain the design of the cavity and the results demonstrating compliance with this requirement.

2. VACUUM SYSTEM, TEMPERATURE STABILITY AND CAVITY FINESSE

2.1 Introduction

In this section we explain how the LISA frequency stability requirements have led to specific design choices for this application. Also, prior to measurements of the frequency stability, we also describe the determination of the cavity finesse via the cavity ringdown time. These measurements were made both before and after mounting of the cavity in a vacuum chamber and subsequent pump-down and were made to confirm that both axes had a finesse of more than our target of 200,000.

2.2 General design considerations

In this section, we discuss the choice of material for the cavity spacer and mirror substrate with focus on the frequency stability specification (see Section 1). The thermal noise limit of a 5-cm cubic cavity with ULE substrate mirrors [4, 5, 6] in terms of a fractional Allan deviation is typically 2×10^{-15} over timescales of a few seconds once the isothermal cavity drift is removed. Lower thermal noise limits are observed with fused silica substrates with the lowest limits observed with crystalline mirror coatings [7]. However, whilst fused silica mirrors give better stability on short timescales, the thermal expansion mismatch with the ULE spacer reduces the temperature at which the linear coefficient of thermal expansion (CTE) is zero, which can be harder to operate at. This will make it more difficult to meet the frequency noise requirements at 2 mHz because better thermal shielding and control will be required. One way to partially correct for the effect of the thermal expansion mismatch, is to optically contact ULE annuli to the reverse surface of the mirrors [8]. The complete cavity assembly might have a CTE = 0 at above room temperature [9] but this will depend on the spacer material properties. Therefore, to be sure of a zero CTE significantly above room temperature, we have chosen to use ULE rather than fused silica mirrors. On short timescales (i.e., for $f \gg 2$ mHz), the white frequency noise limit of 30 Hz/√Hz corresponds to an Allan deviation [10] of $21/\sqrt{\tau}$ Hz which is significantly higher than the cavity thermal noise limit for ULE mirrors. On timescales of a few seconds, this suggests that ULE mirror substrates might be acceptable.

To retain vibration insensitivity in the design of the cube, it is important to use the correct cut-out depth to truncate the vertices of the ULE cubic spacer [1]. This cut-out depth depends on parameters such as the mirror diameter and whether thermal compensating annuli [8] are used. To make the cubic spacer suitable for both ULE and fused silica substrate mirrors, we decided to have the ULE spacer machined on the assumption that annuli would be used. Therefore, even with ULE mirrors, we contacted ULE annuli on the reverse side. Although ULE mirrors allowed us to meet the LISA requirements, we plan to use a second identical spacer to investigate the effect of using fused silica mirrors.

2.3 Thermal shielding and temperature stability

The cavity assembly was mounted within an aluminium vacuum chamber, and two layers of aluminium plates provided passive thermal shielding of the cavity within the chamber. The cavity is held by four PEEK spheres providing Hertzian contacts in a tetrahedral configuration. These spheres act as the mechanical and thermal interface of the cavity with the internal vacuum chamber assembly and, by extension, the external environment. To maximise the cavity stability the plates were polished to a mirror finish and then gold-plated to reduce the thermal emissivity to 0.03 [11] (see Figure 1).

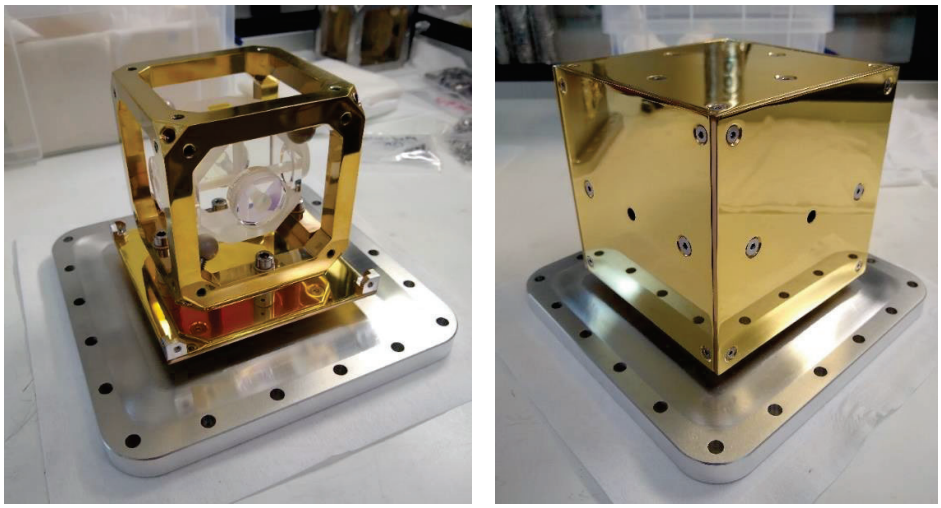

Figure 1: Photographs of the assembled cavity mounted on the vacuum chamber baseplate with (right) and without (left) thermal shield plates

Active thermal control of the cavity system was provided by two polyimide flexible heater pads connected to commercial PID controllers. The controllers provided each pad with up to 18 W of heating power over a 14.4 cm^2 heating area. One pad was fixed to the top of the vacuum chamber, with the other fixed to the underside of the vacuum chamber baseplate. Rubber foam insulation (20 mm thick) was placed around the vacuum chamber to aid the active control and reduce thermal noise at the vacuum chamber outer surfaces.

Figure 2 shows the temperature measured by a PT100 temperature sensor placed next to the heater pad on top of the vacuum chamber. It shows the change in the vacuum chamber surface temperature at this point in response to an input from the controllers to raise the system from ambient to 40 °C from ambient. Fitting an exponential curve to this plot gives a thermal time constant for the outside of the vacuum chamber of approximately 1 hr. The anomaly seen at approximately ~6000s is due to the PID controller exhibiting a small amount of 'overshoot' before settling at a steady-state temperature.

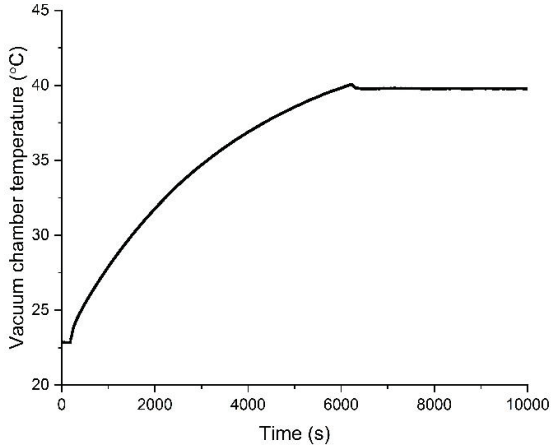

Figure 2: Vacuum chamber surface temperature in response to a step change in controller set temperature at T0. The ambient laboratory temperature was ~23 °C, and the controller target temperature was 40 °C.

To obtain an initial estimate of the thermal time constant of the cubic cavity the thermal response shown in Figure 2 was used as a boundary condition input in a thermal finite element model of the cavity system (see Figure 3). The finite-element model captured the conductive and radiative heating effects inside the vacuum chamber, assuming a perfect vacuum and therefore no convective heating. One-eighth symmetry was used to reduce the computational time with the final model comprising 40,000 solid elements with quadratic Lagrange discretisation. A time-dependent study was conducted to model the temperature of the system for 120 hours after application the experimentally measured vacuum chamber temperatures.

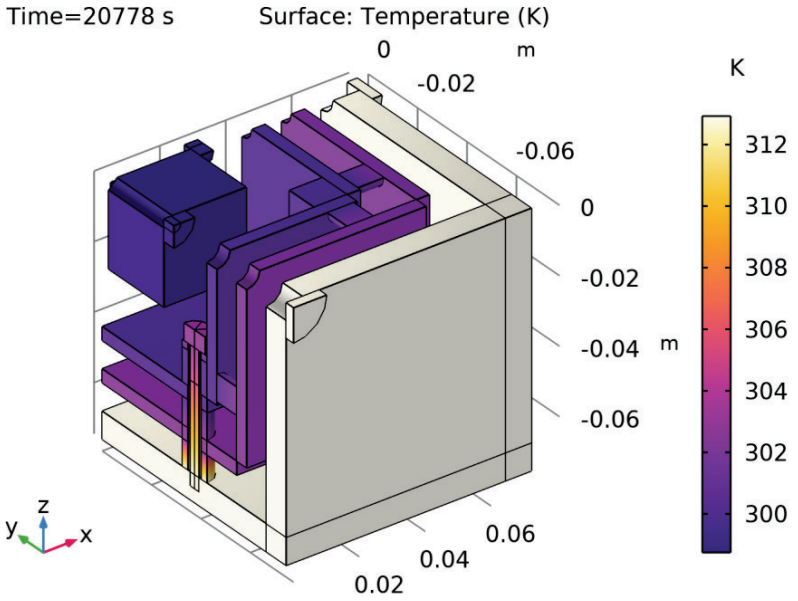

Figure 3: View of the finite-element model showing colour gradient of surface temperatures throughout the layers of the cavity vacuum chamber assembly

Figure 4 shows the average temperature of the cubic cavity as predicted by this model. Again, fitting an exponential curve to the plot gives a thermal time constant for the cubic cavity of approximately 17.8 hrs. This indicates that when the thermal controllers are set to a new temperature the cavity will require at least 48 hrs to settle at this new temperature.

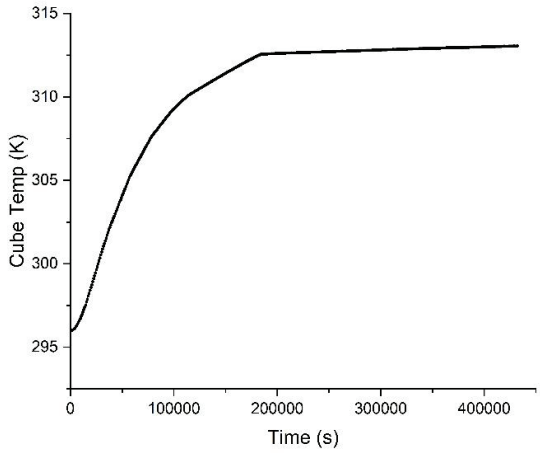

Figure 4: Finite-element model prediction of the average temperature of the cubic cavity in response to a change in the vacuum chamber surface temperatures matching that in Figure 2

2.4 Cavity ring-down time

The cavity finesse was determined by measurement of the cavity ring-down time. Light was coupled into the cavity and the laser tuned so that the frequency of a sideband of an electro-optic modulator was resonant with the cavity TEM00 mode. The RF drive to the modulator was then switched off and the resulting decay of the light transmitted through the cavity measured using a fast detector and digital oscilloscope.

Fitting an exponential decay curve to the ring-down data enables a time constant τ to be determined. The finesse $\mathcal{F}$ can then be calculated from:

$$\mathcal{F} = 2\pi\tau\Delta\nu_{FSR} \tag{3}$$

Here $\Delta\nu_{FSR}$ denotes the cavity free spectral range for the cavity (*i.e.*, 3.0 GHz for a 5 cm cavity). Figure 5 shows decay curves measured from both optical axes, with exponential decay curves fitted giving time constants of 12.8 μs (in Plot A) and 12.2 μs (in Plot B). The manufacturer's quoted finesse value for the mirrors was 200,000 and these time constants correspond to finesse values of 241,000 and 230,000 respectively, indicating a good level of alignment and cleanliness had been achieved during assembly.

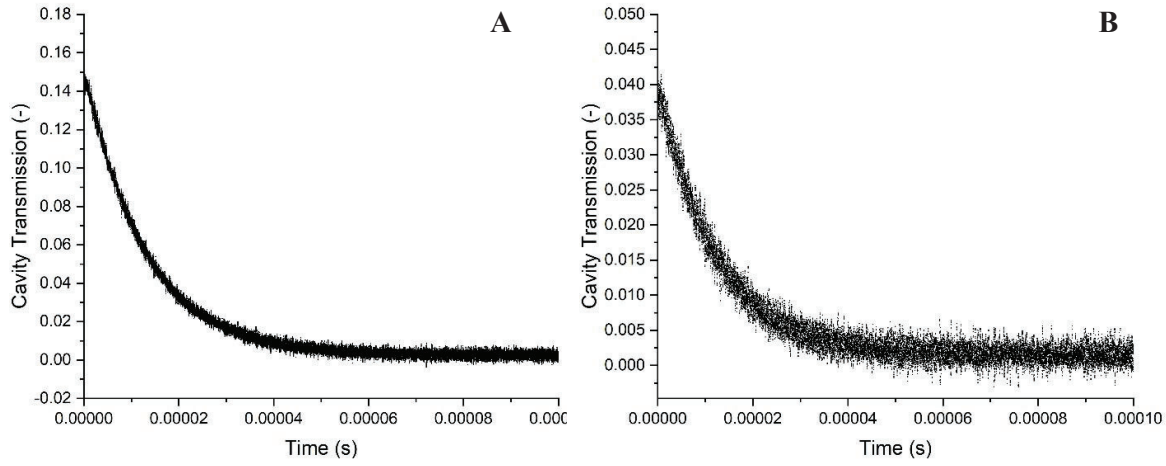

Figure 5: Ring-down measurements for the TEM_{00} mode for both bore #1 (Plot A) and bore #2 (Plot B).

3. FREQUENCY STABILITY MEASUREMENT SYSTEM

3.1 Reference laser

The frequency stability of a 1064-nm laser locked to the cavity along one bore of our dual axis cubic cavity was measured versus an NPL ultra-stable laser system by beat frequency comparison. Measurements of the frequency stability of a Mephisto laser locked to the NPL cubic cavity were undertaken by beat frequency comparison versus an independent NPL cavity-stabilised laser at 1064 nm (Figure 6). This ultra-stable 48-cm long cavity [12] is mounted within a 3-layer thermal shield. It has a typical measured drift rate of 20 mHz/s, but the light sent via fibre to our test laboratory is also drift-corrected by reference to an NPL maser signal so that the residual frequency drift of the 48-cm cavity is reduced to less than 100 μHz/s [13]. Phase noise introduced by thermal and mechanical fluctuations in the fibre link from the reference laser is compensated using a scheme similar to that reported in [14].

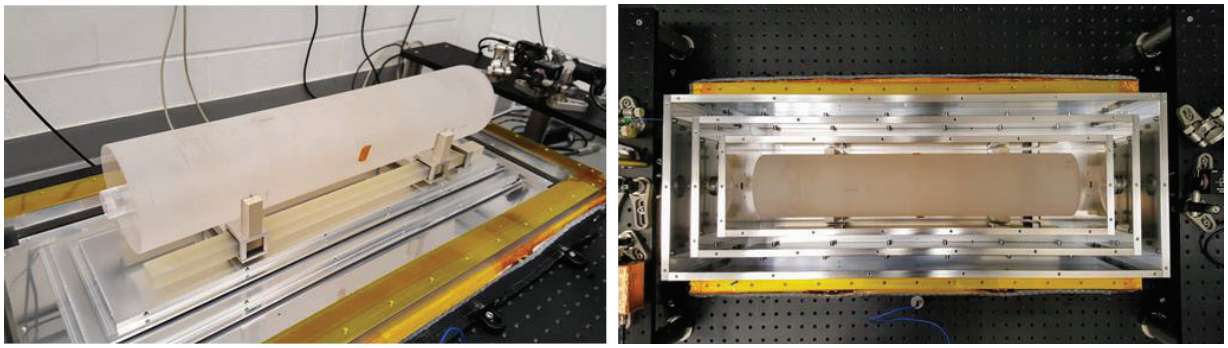

Figure 6**:** NPL 48-cm long cavity to be used as a frequency reference for comparison against the LISA cubic cavities

3.2 Beat frequency system

The beat frequency arrangement is shown in Figure 7. A frequency counter is interfaced to a laptop via a GPIB to USB converter; this counter is NPL maser referenced to avoid uncertainty arising from frequency drift in the counter internal oscillator.

NPL-written software allows the option of data transfer point by point to monitor the beat frequency or to collect the results with zero dead-time between measurements. Up to one million results can be stored in the counter and transferred to the PC once data-taking is complete. For measurements of frequency stability (*i.e.*, frequency noise PSD, or power spectral density) it is critical that results have zero dead-time [15]. A zero dead time is also important in understanding the effect of fibre link temperature variations on frequency noise PSD. However, for other applications (*e.g.*, measurement of the thermal expansion) it can be more helpful to obtain and display the results in real time. However, in this latter case, there is necessarily a dead time between readings of typically a few ms whilst the PC reads the counter.

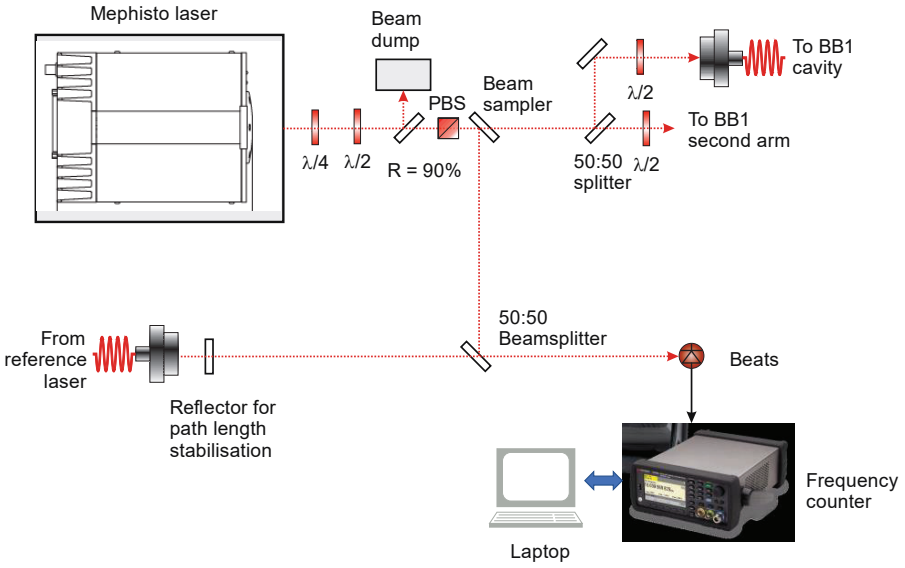

Figure 7: Schematic for determining the frequency stability of a cavity stabilised Nd:YAG laser at 1064 nm by beat frequency measurement versus a reference laser

The measured beat f_{beat} is given by:

$$f_{beat} = f_{LISA} - f_{NPL} \tag{4}$$

Here, f_{LISA} is the Mephisto laser frequency when locked to an arm of the cubic cavity and f_{NPL} is the frequency of the NPL reference laser. The beat sign was established by tuning the Mephisto laser and a prior determination using a wavemeter of the dependency of the Mephisto laser frequency on operating temperature. The direction of the frequency tuning was compared with the tuning of the beat to determine the sign. The results presented in this report all relate to the Mephisto laser locked to a spatial TEM_{00} mode. This was verified by using a camera to determine the spatial mode pattern transmitted through the cavity.

4. LISA CAVITY FREQUENCY MEASUREMENTS

In this section we give the main results that characterise our dual-axis cubic cavity. Prior to measurements of frequency stability, we determined the finesse of both bores of our DACC, and these results are shown in section 2.4. Our determination of the thermal expansion of both cavity bores is described in section 4.1 and the results are used to decide on the cavity operating temperature and the choice of bore. Section 4.2 shows the results from our determination of the cavity thermal time constant following a step change in set temperature. Section 4.3 gives the main results of the determination of the frequency noise power spectral density (PSD) of a laser locked to this cavity. Finally, section 4.4 gives results that show the contribution to the frequency noise PSD from thermal variations in a fibre link.

4.1 Cavity thermal expansion

For bore #1, the beat frequency reduces as the laser temperature increases and so $f_{LISA} > f_{NPL}$. At the temperature where the linear thermal expansion is zero, we expect that the cavity length is at a minimum. The variation of beat frequency as a function of temperature is therefore expected to follow:

$$f = f_0 - \alpha(T - T_0)^2 \tag{5}$$

Here, f_0 is the beat frequency at the temperature T_0 where the linear thermal expansion is zero; α is the quadratic expansion coefficient.

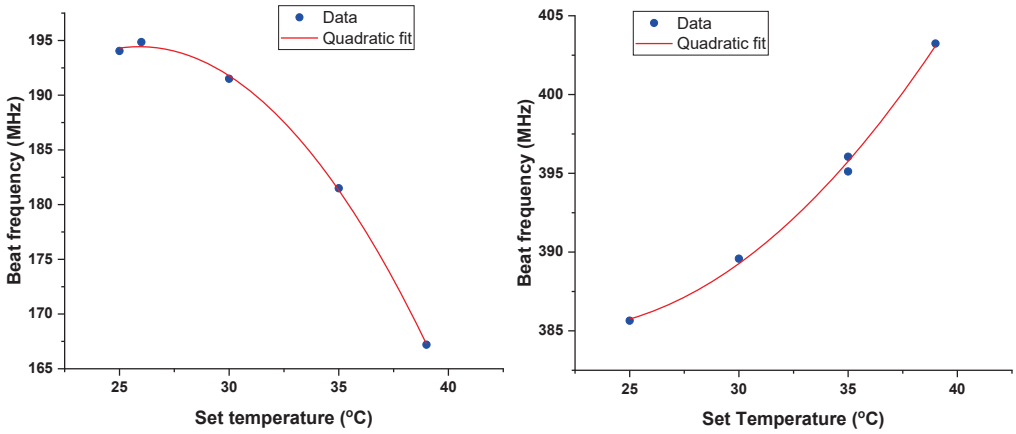

Figure 8: Variation of the beat frequency as a function of temperature for a laser locked to bore #1 (Figure 8a, left) and bore #2 (Figure 8b, right)

The LISA cubic cavity is temperature controlled via a pair of commercially available controllers; one controls a heater pad on the top vacuum chamber surface and the second controls the lower surface. Both are set to the same temperature, and it is this common temperature as read by the controller that is reported here.

For one bore (bore #1), we fit the data to a quadratic to obtain T_0 = 25.9 °C and α = 0.158 MHz/K^2. For the orthogonal bore (bore #2), we find that $f_{LISA} < f_{NPL}$ which inverts the parabola (Figure 8b) and gives T_0 = 21.6°C and α = 0.0594 MHz/K^2. The difference in thermal properties of ULE in different directions was reported in [2] and is a result of material anisotropy. Since bore #1 has the higher crossover temperature, most of the results reported here relate to bore #1 operated at a set point temperature of 26°C.

4.2 Cavity thermal time constant

In cycling the cavity temperature to produce the thermal expansion plots of Figure 8 we were also able to determine the cavity thermal time constant. For this measurement, the beat frequency between our laser and the NPL reference was recorded once every second. These beat frequency results f were then converted to an effective temperature T using the results from section 4.1 which gives the relationship as:

$$T = T_0 + \sqrt{\frac{f_0 - f}{\alpha}} \tag{6}$$

In the above equation, α = 0.158 MHz/K^2; this relates to the thermal expansion for bore #1. The cavity set-point temperature T can then be fitted to an exponential of the form:

$$T = T_0 - A \exp\left(-\frac{t}{\tau}\right) \tag{7}$$

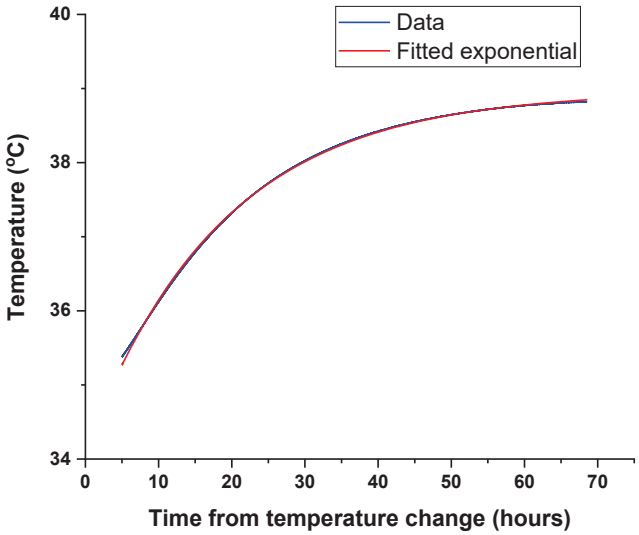

Figure 9: Measurement of the thermal time constant of the cubic cavity following correction of the beat frequency data using the known non-linearity of the cavity thermal expansion.

Fitting (as shown in Figure 9) yields t = 18.4 hours which compares extremely well with the modelled time constant of 17.8 hours (see Section 2.3).

4.3 Frequency noise power spectral density

In this section we discuss our measurements of the frequency noise power spectral density (PSD). According to the LISA specified requirements the PSD ($º\ S_n(f)$) is given by:

$$\sqrt{S_v(f)} \leq 30 \frac{Hz}{\sqrt{Hz}} \sqrt{1 + \left(\frac{2\ mHz}{f}\right)^4} \tag{8}$$

This is required over the frequency range 0.1 mHz < f < 1 Hz. Sets of time-series beat frequency results were taken with a maser-referenced frequency counter set to a 0.5 s gate time in zero dead-time mode [15]. The 0.5 s gate time is required to allow calculation of the frequency noise PSD to 1 Hz.

Prior to these measurements, the PDH lock RF phase difference between the modulation frequency sent to the laser and to the double balanced mixer was optimised. Also, the AC gain of the photodetector was adjusted and the power into the cavity reduced to a few tens of μW to minimise the contribution of thermal noise to the frequency instability arising from the mirrors.

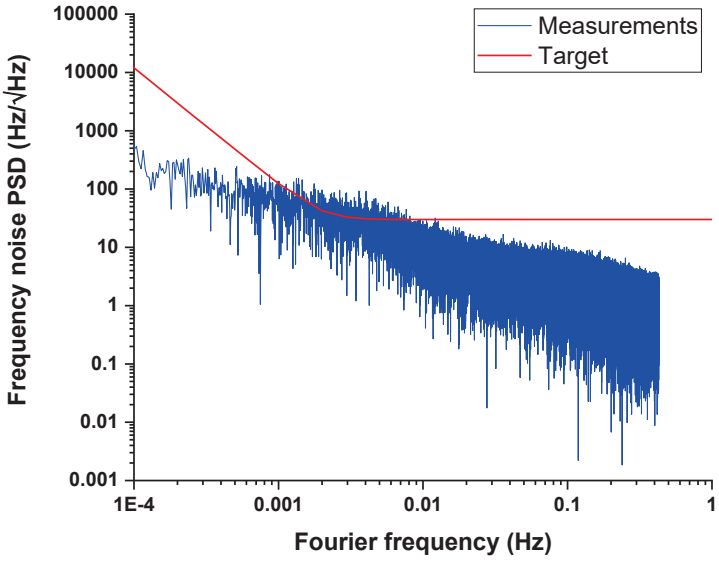

Figure 10: Measurement of the frequency noise power spectral density of a laser locked to bore #1 of the NPL cubic cavity. Results were calculated from time-series beat frequency data taken continuously over ~3 days.

Prior to calculation of the frequency noise PSD, the beat frequency data was corrected for the linear drift rate of 0.2 Hz/s; this rate is expected to reduce over time following initial pump-down. The frequency noise PSD was calculated from the time series beats data via an FFT using a rectangular window and is shown in Figure 10. The cavity performance meets the LISA target, although this performance is marginal at the most demanding part of the frequency range of 2 mHz or (500 s).

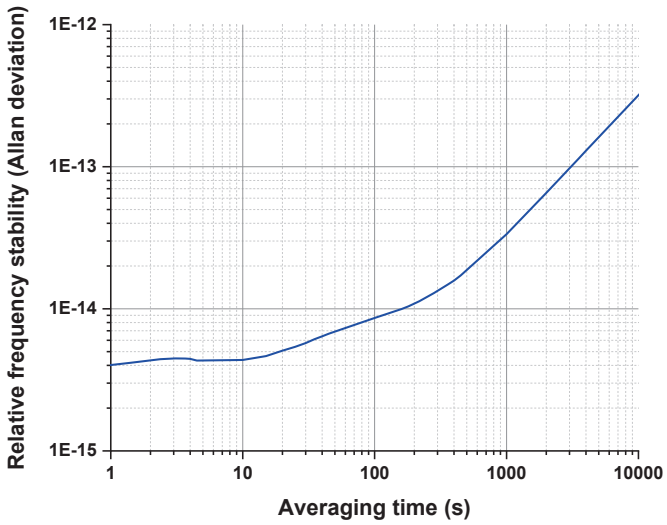

Figure 11: Frequency stability data of a laser locked to bore #1 of the NPL cubic cavity (Figure 10) calculated as an Allan deviation. Results were calculated from time-series beat frequency data taken continuously over ~3 days

The time series beat frequency data used to calculate the above plot can also be used to evaluate the Allan deviation [16]. Following removal of the cavity isothermal drift, the Allan deviation (Figure 11) is independent of measurement time over timescales between 1 and ~20 s, indicating flicker noise. This is consistent with the plot in Figure 10 which shows that on these timescales, the frequency noise PSD $\sqrt{S_v(f)}$ reduces as $1/\sqrt{f}$. Although well within the LISA specification on these timescales we note that the observed flicker noise could be further reduced to the thermal noise limit of ~2 x 10^{-15} [4, 5, 6]. In our setup for example, the lock error signal to noise ratio could be improved by increasing the modulation index but we chose not to do this since an additional amplifier would increase the overall device heat load.

4.4 Temperature variations of a fibre link between the laser and cavity

For the laser to meet the frequency noise power spectral density requirements, it is important that the phase noise introduced by a fibre link between the laser and cavity does not introduce sufficient noise that the complete system exceeds the LISA specification. This induced fibre phase noise could, of course, be corrected for [14] but, to keep the optical setup as simple as possible, there is a strong preference not to have to implement this. The induced frequency noise could be reduced either via a shorter fibre link or additional thermal insulation along the fibre.

Understanding the effect of temperature variations of a fibre link requires a reliable measurement of the variation of refractive index (n) with temperature (T). At a wavelength of 1 μm and at 300 K, one group [17] gives a figure (in their table 6) of dn/dT = 8.6 × 10^{-6} K^{-1} for Corning 7980 bulk fused silica. Also, over the wavelength region 405 nm – 668 nm, a different group [18] gives a maximum figure of dn/dT = 9 × 10^{-6} K^{-1} for "commercial fused silica". Finally, measurements on optical fibres have been reported by a Chinese group [19] at 633 nm; this is dn/dT = 7.8 × 10^{-6} K^{-1}; this number is from some prior experimental work (reference 17 in their paper), but this figure agrees reasonably well with their theory. In view of the variation of figures in the literature, we have made an independent measurement of dn/dT for our fibre link. This temperature dependency was measured by sandwiching a 3 m length of fibre between a Peltier and thin metal plate. The fibre spool was temperature controlled and set point could be varied by applying an external voltage input. The applied temperature ramp was set to be ~0.02 Hz and the fibre temperature was sampled at via a pair of thermistors. Attempting to apply much faster temperature ramps was not possible owing to the thermal time constant of the overall setup. However,

aiming for slower temperature variations leads to smaller frequency variations. This is because, as explained later, thermal noise in the fibre link leads to optical phase noise; the differential of this yields the expected frequency noise.

Two datasets were taken, with some repositioning of the monitor thermistors between measurements. One of these two datasets, where the thermistors measured a temperature amplitude of 1.6 K, is shown in Figure 12. These results were obtained by beat frequency comparison versus the NPL reference laser using our frequency counter with a 100 ms gate time, operating in zero dead time mode.

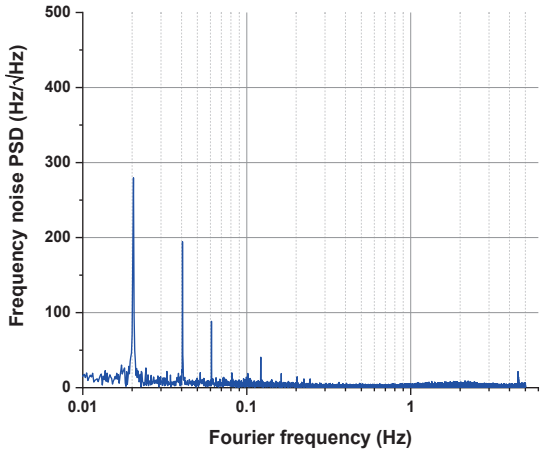

Figure **12**: Observed frequency noise PSD on a laser locked to the cubic cavity with thermal noise at 0.02 Hz induced in the 2.8 m fibre between the laser and cavity

To interpret the results of Figure 12, we outline the effect on laser phase noise and explain how this is converted to frequency noise. The phase noise ϕ_n induced in a fibre of length L and for a laser at a wavelength of λ = 1064 nm is:

$$f_n = \frac{2\pi L}{\lambda}\frac{\partial n}{\partial T} \tag{9}$$

To obtain the frequency noise, we write [16]:

$$S_f(\omega) = \omega S_f(\omega) \tag{10}$$

This gives the angular frequency spectral noise density, and we need to divide by 2π to get the frequency spectral noise density. Using a figure of $dn/dT = 9 \times 10^{-6}$ K^{-1} and the above equations over 2.8 m (Figure 12), we get an induced phase variation of 266 rad/K. At 0.02 Hz, this yields an expected frequency variation of 3 Hz/K. The results in Figure 12 show a frequency noise peak of 280 Hz/√Hz and this results from a 1.6 K amplitude temperature oscillation at 0.02 Hz. To convert the frequency noise peak of Figure 12 to a frequency amplitude, we multiply by $\sqrt{(2\delta n)}$ where δn is the FFT bandwidth. In this figure, the bandwidth is 0.000185 Hz which results from the total measurement period of 5400 s. The noise peak of 280 Hz/√Hz therefore corresponds to a frequency amplitude of 5.4 Hz and a sensitivity of 3.4 Hz/K. Taking the mean of this and a second determination of this coefficient give us a final value over 2.8 m of $dn/dT \sim 1.2 \times 10^{-5}$ K^{-1}.

The proposed fibre length in the final system is 5 m and the frequency stability needs to be achieved within an environment where the thermal noise in K/√Hz is given by:

$$\sqrt{S_T(f)} = 0.1\frac{K}{\sqrt{Hz}}\sqrt{1+\left(\frac{20\ mHz}{f}\right)^4} \tag{11}$$

The equation for the thermal noise given by the formula above therefore contributes the following to the frequency noise:

$$\sqrt{S_n(f)} = 35.4\ \times f \times \frac{Hz}{\sqrt{Hz}}\sqrt{1+\left(\frac{20\ mHz}{f}\right)^4} \tag{12}$$

This is required over the frequency range 0.1 mHz < f < 1 Hz; a comparison over this frequency range between thermally induced fibre noise and the LISA specification is shown in Figure 13.

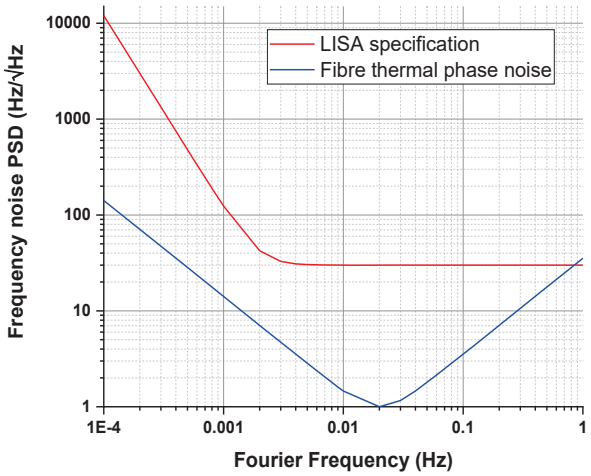

Figure **13**: Comparison over this frequency range between thermally induced fibre noise and the LISA specification using the fibre temperature sensitivity determined in this study

As observed in Figure 13, thermally induced fibre phase noise is primarily a problem at 1 Hz. The specification at 1 Hz is 30 Hz/√Hz whereas using our experimentally determined value for the fibre temperature dependency the frequency noise PSD contribution from the fibre will be 35 Hz/√Hz. However, with some additional thermal insulation, we can expect that it should be straightforward to meet the LISA requirements without fibre phase noise cancellation.

5. SUMMARY

The design and testing of a laser frequency stabilisation system for potential use in the LISA mission has been presented. This system has been characterised and found to have mirror finesse values ≥ 230,000, a cavity thermal time constant of ~18 hrs, and CTE-zero temperatures for the optical axes of 25.9 °C and 21.6 °C. The system frequency stability has also been shown to be capable of meeting the LISA mission frequency noise requirements. Finally, the effects of thermally induced phase noise in the optical fibres have also been investigated, showing good performance against the LISA specifications, and indicating that with some minor thermal insulation the system would not need to implement phase noise cancellation methods.

ACKNOWLEDGEMENTS

We acknowledge funding from the European Space Agency under contract 4000132072/20/NL/IB/ig. We also wish to thank Ian Hill and Ben Allen for assistance with the cavity finesse measurements, Marco Schioppo for photographs of the NPL reference cavity (Figure 6) and Billy Robertson for assistance with the vacuum chamber assembly.

REFERENCES

[1] S. Webster and P. Gill, "Force-insensitive optical cavity," *Optics Letters,* vol. 36, no. 18, pp. 3572-3574, 2011.

[2] I. R. Hill, R. J. Hendricks, S. Donnellan, P. Gaynor, B. Allen, G. P. Barwood and P. Gill, "Dual-axis cubic cavity for drift-compensated multi-wavelength laser stabilisation," *Optics Express,* vol. 29, p. 36758, 2021.

[3] R. Sütterlin, G. P. Barwood, G. Cole, C. Deutsch, P. Gaynor, D. Gerardi, M. Ghulinvan, P. Gill, C. Greve, R. J. Hendricks, I. R. Hill, S. Koller, S. Kundermann, R. Le Goff, S. Lecomte, C. Meier, S. Schilt, C. Stenzel, K. Voss and A. Zhukov, "Towards space deployable laser stabilisation systems based on 5-cm vibration insensitive cubic cavities," in *Joint Conference of the European Frequency and Time Forum and IEEE International Frequency Control Symposium*, 2021.

[4] K. Numata, A. Kemery and J. Camp, "Thermal noise limit in frequency stabilization of lasers with rigid cavities," *Phys Rev Lett,* vol. 93, p. 250602, 2004.

[5] M. Notcutt, L.-S. Ma, A. D. Ludlow, S. M. Foreman, J. Ye and J. L. Hall, "Contribution of thermal noise to frequency stability of rigid optical cavity via Hertz-linewidth lasers," *Phys Rev a,* vol. 73, p. 031804(R), 2006.

[6] G. Xu, D. Jiao, L. Chen, L. Zhang, R. Dong, T. Liu and J. Wang, "Thermal Noise in Cubic Optical Cavities," *Photonics,* vol. 8, no. 7, p. 261, 2021.

[7] G. D. Cole, W. Zhang, M. J. Martin, J. Ye and M. Aspelmeyer, "Tenfold reduction of Brownian noise in high-reflectivity optical coatings," *Nature Photonics,* vol. 7, pp. 644-650, 2013.

[8] T. Legero, T. Kessler and U. Sterr, "Tuning the thermal expansion properties of optical reference cavities with fused silica mirrors," *Journal of the Optical Society of America B,* vol. 27, no. 5, pp. 914-919, 2010.

[9] J. Sanjuan, K. Abich, M. Gohlke, A. Resch, T. Schuldt, T. Wegehaupt, G. P. Barwood, P. Gill and C. Braxmaier, "Long-term stable optical cavity for special relativity tests in space," *Optics Express,* vol. 27, no. 25, pp. 36206-36220, 2020.

[10] D. W. Allan, "Should the Classical Variance Be Used As a Basic Measure in Standards Metrology?," *IEEE Trans Instrum Meas,* Vols. IM-36, pp. 647-654, 1987.

[11] Omega Engineering Inc., "Emissivity of Common Materials," [Online]. Available: https://www.omega.co.uk/literature/transactions/volume1/emissivitya.html.

[12] M. Schioppo, J. Kronjäger, A. Silva, R. Ilieva, J. W. Paterson, C. F. A. Baynham, W. Bowden, I. R. Hill, R. Hobson, A. Vianello, M. Dovale-Álvarez, R. A. Williams, G. Marra, H. S. Margolis, A. Amy-Klein, O. Lopez, E. Cantin, H. Álvarez-Martínez, R. Le Targat, P. E. Pottie, N. Quintin, T. Legero, S. Häfner, U. Sterr, R. Schwarz, S. Dörscher, C. Lisdat, S. Koke, A. Kuhl, T. Waterholter, E. Benkler and G. Grosche, "Comparing ultrastable lasers at 7 × 10^17 fractional frequency instability through a 2220 km optical fibre network," *Nature Communications,* vol. 13, p. 212, 2022.

[13] M. Schioppo, private communication, 2022.

[14] L.-S. Ma, P. Jungner, J. Ye and J. L. Hall, "Delivering the same optical frequency at two places: accurate cancellation of phase noise introduced by an optical fiber or other time-varying path," *Optics Letters,* vol. 19, pp. 1777-9, 1994.

[15] P. Lesage and C. Audoin, "Effect of Dead-Time on the Estimation of the Two-Sample Variance," *IEEE Trans Instrum Meas,* Vols. IM-28, pp. 6-10, 1979.

[16] D. W. Allan, "Statistics of Atomic Frequency Standards," *Proc IEEE,* vol. 54, pp. 221-230, 1966.

[17] D. B. Leviton and J. F. Bradley, "Temperature dependent absolute refractive index measurements of synthetic fused silica," *Proc SPIE (Optomechanical Technologies for Astronomy, 62732K),* vol. 6273, 2006.

[18] R. M. Waxler and G. W. Cleek, "Refractive Indices of Fused Silica at Low Temperatures," *Journal of Research of the National Bureau of Standards-A. Physics and Chemistry,* vol. 75A, pp. 279-281, 1971.

[19] W. Zhi-Yong, Q. Qiu and S. Shuang-Jin, "Temperature dependence of the refractive index of optical fibers," *Chinese Physics B,* vol. 23, no. 3, p. 034201, 2014.